Research Article

Finite-Element Analysis on Compressive Performance of a Novel Glue-Laminated Cornstalk Scrimber

Wei Tian ⓘ, Yongmei Qian ⓘ, Zunpeng Liu ⓘ, and Yiming Wang ⓘ

Jilin Jianzhu University, Changchun 130118, China

Correspondence should be addressed to Yongmei Qian; qianyongmei@jlju.edu.cn

Novel glue-laminated cornstalk scrimber is a new timber substitute produced by special techniques, without damaging the original fibers in cornstalks. This novel material outperforms ordinary timber in the resistance to water, damping, insect, and fire and provides a desirable green building material. However, glue-laminated cornstalk scrimber has not been widely implemented in the building industry, because the application of cornstalk products is limited to decoration panels. With the aid of the finite-element software Abaqus, this paper simulates the glue-laminated cornstalk scrimber specimens with different slenderness ratios under axial compression and analyzes the compressive performance of such specimens. The results show that the height of glue-laminated cornstalk scrimber is negatively correlated with the buckling load and nonlinear load under axial compression and positively correlated with the transverse displacement and axial displacements induced by axial compression. The research results provide a good reference for improving the design and application of glue-laminated cornstalk scrimber.

1. Introduction

Konjac is a perennial herbaceous plant in the genus of *Amorphophallus*, Araceae family. The main active component is konjac glucomannan (KGM), a water-soluble natural polymer polysaccharide [1]. The KGM is generally considered as a polysaccharide formed by linking glucose and mannose at the ratio of $1:1.69$ or $1.4:1$ through β-1, 4 glycosidic bonds. With a molecular weight of 200–$20,000$ kDa, the KGM has an acetyl group at the C6 position for every 19 sugar units on the main chain [2, 3].

In recent years, China has highlighted the importance of ecological civilization and further restricted timber consumption to protect forest resources. As a result, a diverse array of timber substitutes has emerged, such as scrimber and glulam [1, 2].

Much research has been done on timber substitutes around the world. For instance, Uzel et al. [3] compared the flexural behavior of glulam beams with that of large-volume timber beams. The University of Catania [4] described the structural behaviors of glued laminated (GL) timber and laminated veneer lumber (LVL) and introduced a new

technique called post-tensioning of timber beams. Through tests and evaluation, Graz University of Technology [5] proposed a generic design approach generally applicable for all linear and planar, unidirectional, and orthogonal laminated structural timber products. The Institute for Mechanics of Materials and Structures [6] developed a stochastic engineering framework capable of accounting for how the random fluctuations of the stiffness of wooden boards work on the performance of glued laminated timber (GLT). Anshari and Guan [7] established a finite-element model to simulate the prestress performance of compressed wood (CW) glulam beams and further examined the structural properties of prestressed beams under destructive bending.

Cornstalks, the most common type of crop stalks, can be reconstituted and recombined into a novel timber substitute. This helps to protect the air environment and alleviate the shortage of forest resources. Therefore, the application of glue-laminated cornstalk scrimber not only boasts profound theoretical value but also has great economic and social significance [8–10]. Despite its excellent features (e.g., high density, high strength, fire resistance, corrosion resistance,

moisture resistance, and insect resistance), glue-laminated cornstalk scrimber has only been applied as decorative panels. Few studies have attempted to implement the novel material in the building industry [11–14].

In the light of the above, this paper carries out a finite-element simulation on the compressive performance of glue-laminated cornstalk scrimber, shedding theoretical new lights on the mechanical performance of this novel material. The research results could promote the design and application of glue-laminated cornstalk scrimber.

2. Finite-Element Analysis on Glue-Laminated Cornstalk Scrimber under Axial Compression

2.1. Constitutive Relationship. Glue-laminated cornstalk scrimber is a nonsymmetrical anisotropic material. To measure its compressive performance, the elastic moduli, Poisson's ratios, and shear moduli of three surfaces were recorded in the elastic phase: the fiber direction 1, the scrimber direction 2, and the bonding direction 3. Referring to the definitions of timber yield phase, the generalized Hill yield criterion [15–19] was introduced for the yield phase. Table 1 lists the performance parameters of glue-laminated cornstalk scrimber.

2.2. Finite-Element Model. The axial compression specimens of glue-laminated cornstalk scrimber were meshed into three-dimensional (3D) eight-node hexagonal elements C3D8R (Figure 1). The load was applied concentratedly on the top of the specimen. The load was fixed for the elastic model and gradually stepped up for the nonlinear model. At the bottom of the specimen, the support was allowed to rotate in one direction only; at the top, the support could rotate in one direction and displace in the axial direction. Through structural optimization, the finite-element model of glue-laminated cornstalk scrimber mainly consists of hexagonal elements [20, 21].

2.3. Model Size. This research only considers the overall stable bearing capacity, without tackling local stability. Therefore, the slenderness ratio of the finite-element model was changed to study its effect on the ultimate bearing capacity.

Drawing on Technical Code of Glued Laminated Timber Structures (GBT50708-2012) and Code for Design of Timber Structures (GB50005-2017), the model size was designed as follows: the sectional area was fixed at 150 mm × 150 mm, while the length was set to 1,200 mm, 1,600 mm, 2,000 mm, 2,400 mm, and 2,800 mm, respectively. The resulting specimens were coded Z-1 to Z-5 in turn (Table 2).

2.4. Results Analysis

2.4.1. Eigenvalue Buckling Analysis. The eigenvalue buckling analysis aims to calculate the ultimate load that drives an elastic member from a stable state to the critical state of instability. The analysis results are consistent with the classical Euler solution. Through Abaqus calculation, the

TABLE 1: The performance parameters of glue-laminated cornstalk scrimber

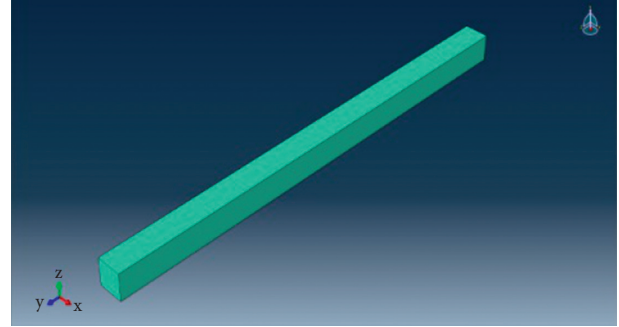| Elastic modulus (MPa)			Shear modulus (MPa)			Poisson's ratio			Density (kg/m^3)
E_1	E_2	E_3	G_{12}	G_{13}	G_{23}	μ_{12}	μ_{13}	μ_{23}	ρ
8.817	925	548	805	584	183	0.21	0.45	0.43	1220

FIGURE 1: The finite-element model of glue-laminated cornstalk scrimber under axial compression.

cloud atlas of buckling equivalent stresses and buckling equivalent displacements of Z-1 to Z-5 were obtained (Figures 2 and 3).

As shown in Figures 2 and 3, the buckling equivalent stress mainly concentrated in the middle of the specimens under axial compression. When the sectional area was fixed, Z-5 had the greatest deflection under ultimate load, while Z-1 had the smallest deflection. The deflection of the axial compression specimen gradually increased with the growth in specimen height. From Z-1 to Z-5, the eigenvalue buckling load was 605 kN, 545 kN, 526 kN, 502 kN, and 456 kN, respectively.

2.4.2. Nonlinear Buckling Analysis. The five axial compression specimens were subject to nonlinear analysis. In this way, the nonlinear buckling load of Z-1 to Z-5 was obtained as 564 kN, 523 kN, 504 KN, 465 kN, and 425 kN, respectively. As shown in Figure 4, the nonlinear buckling load was slightly smaller than the eigenvalue buckling load; the two loads exhibited roughly the same trend: the greater the slenderness ratio, the smaller the load and the weaker the resistance to lateral displacement.

As shown in Figures 5 and 6, for Z-1 to Z-5, the transverse displacement and axial displacements changed similarly under compression load: both of them gradually increased with the load and with the slenderness ratio. In other words, the bearing capacity decreased with the growing load and slenderness ratio. In the early phase of loading, transverse displacement and axial displacements increased almost linearly; the transverse displacement had the greater increasing rate. Later, as the load continued to grow, the traverse displacement tended to be stable, while the axial displacement still exhibited a linear growth.

TABLE 2: The model size.

Specimen number	Sectional area (mm^2)	Length (mm)	Slenderness ratio
Z-1		1200	27.7
Z-2		1600	37.0
Z-3	150 × 150	2000	46.2
Z-4		2400	54.2
Z-5		2800	63.2

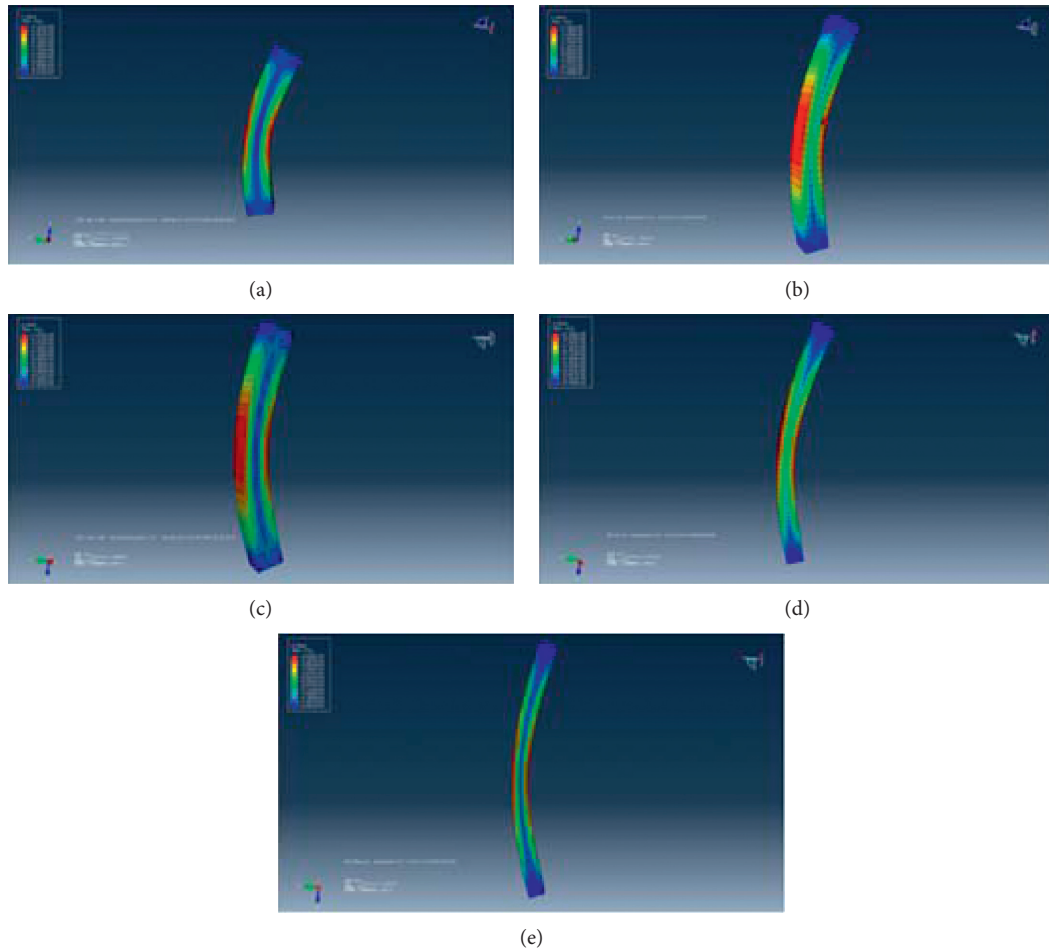
(a)

(b)

(c)

(d)

(e)

FIGURE 2: The cloud atlas of buckling equivalent stresses.
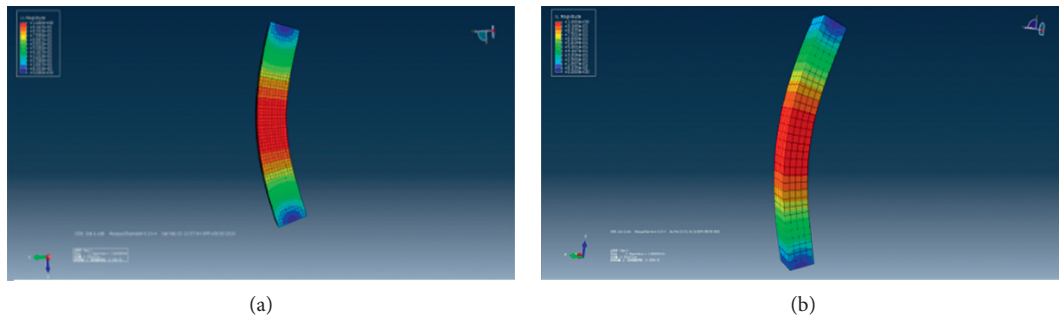

(a)

(b)

FIGURE 3: Continued.
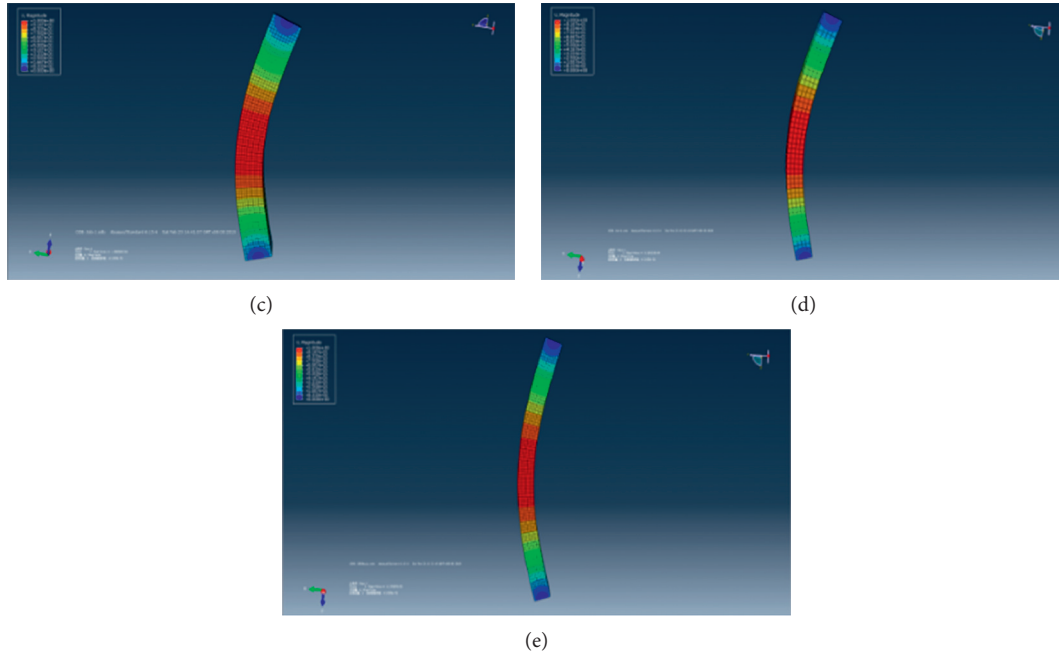
(c)

(d)

(e)

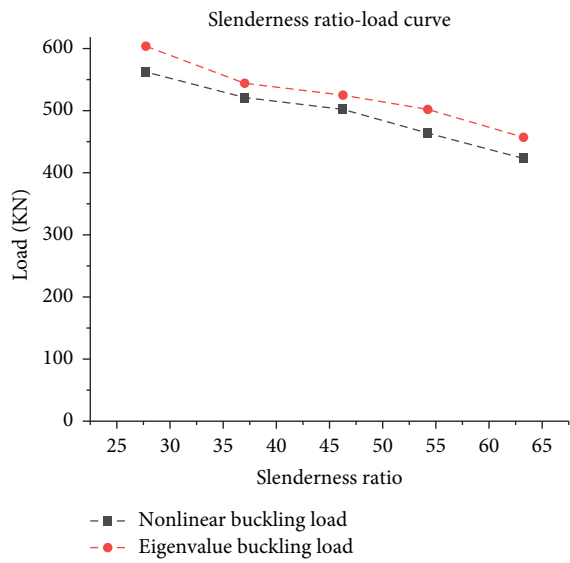FIGURE 3: The cloud atlas of buckling equivalent displacements.
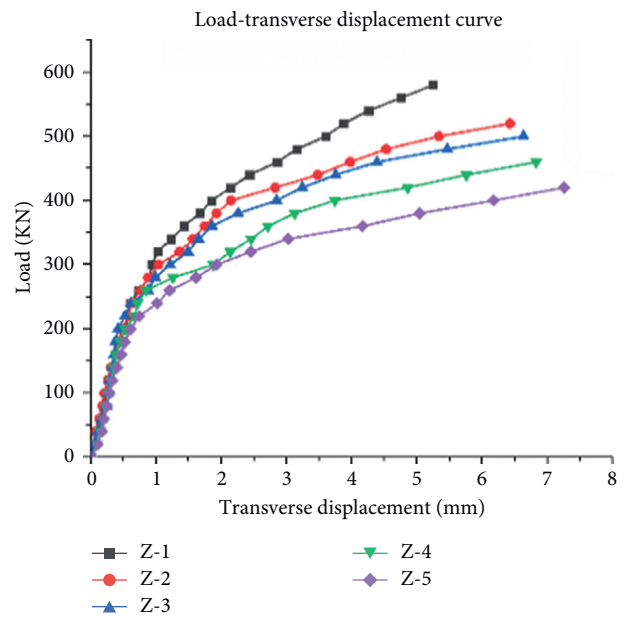

FIGURE 4: The slenderness ratio-load curves.

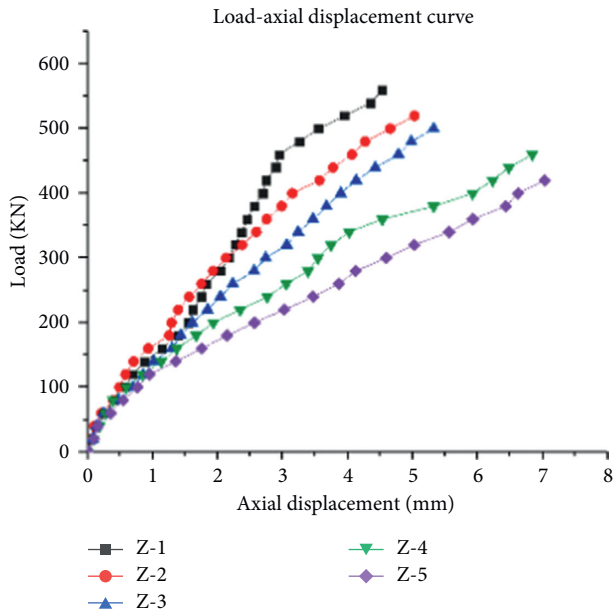FIGURE 5: The load-transverse displacement curves.

FIGURE 6: The load-axial displacement curves.

3. Conclusions

This paper carries out Abaqus finite-element simulation of glue-laminated cornstalk scrimber specimens with different slenderness ratios under axial compression. The generalized Hill yield criterion was introduced for elastoplastic analysis, in view of the nonlinear property of the material; through eigenvalue and nonlinear buckling analyzes, the cloud atlas of buckling equivalent stress and displacement and nonlinear load-displacement curves were obtained. The main conclusions are as follows:

(1) With the growing slenderness ratio, both eigenvalue buckling load and nonlinear buckling load gradually decreased, and the former was slightly greater than the latter. The eigenvalue buckling analysis assumes that the specimens are ideal elastic members, while the nonlinear buckling analysis considers the initial defects of the members. Therefore, the nonlinear buckling analysis better conforms to the actual situation and outputs more reliable results.

(2) According to the nonlinear buckling load-displacement curves, both transverse displacement and longitudinal displacements gradually increased with slenderness ratio. In the early phase of loading, transverse displacement and axial displacements increased almost linearly; the transverse displacement had the greater increasing rate. With further growth of the load, the traverse displacement tended to be stable, while the axial displacement continued to increase linearly at the original rate.

(3) The buckling load and nonlinear load of the axial compression specimens gradually decreased with the growth in specimen height. Moreover, the transverse displacement and axial displacements changed similarly under axial compression: both of them gradually increased with the height of specimen.

Data Availability

The data used to support the findings of this study are available from the corresponding author upon request.

Conflicts of Interest

The authors declare that they have no conflicts of interest.

References

[1] G. B. Hu, Z. T. Zhang, and X. B. Xiao, "China import wood situation and developing trend," *Forest Industry*, vol. 42, no. 1, pp. 5–9, 2015.

[2] X. Sun, M. He, and Z. Li, "Novel engineered wood and bamboo composites for structural applications: state-of-art of manufacturing technology and mechanical performance evaluation," *Construction and Building Materials*, vol. 249, Article ID 118751, 2020.

[3] M. Uzel, A. Togay, Ö. Anil, and C. Sogutlu, "Experimental investigation of flexural behavior of glulam beams reinforced with different bonding surface materials," *Construction and Building Materials*, vol. 158, pp. 149–163, 2018.

[4] A. D'Aveni and G. D'Agata, "Post-tensioned timber structures: new perspectives," *Construction and Building Materials*, vol. 153, pp. 216–224, 2017.

[5] R. Brandner, "Cross laminated timber (CLT) in compression perpendicular to plane: testing, properties, design and recommendations for harmonizing design provisions for structural timber products," *Engineering Structures*, vol. 171, pp. 944–960, 2018.

[6] G. Kandler, M. Lukacevic, C. Zechmeister, S. Wolff, and J. Füssl, "Stochastic engineering framework for timber structural elements and its application to glued laminated timber beams," *Construction and Building Materials*, vol. 190, pp. 573–592, 2018.

[7] B. Anshari and Z. Guan, "FE modelling of optimization on strengthening glulam timber beams by using compressed wood blocks," *Procedia Engineering*, vol. 171, pp. 857–864, 2017.

[8] D. S. Huang, A. P. Zhou, and Y. L. Bian, "Experimental and analytical study on the nonlinear bending of parallel strand bamboo beams," *Construction and Building Materials*, vol. 44, pp. 585–592, 2013.

[9] A. K. Ray, S. Mondal, S. K. Das, and P. Ramachandrarao, "Bamboo-A functionally graded composite-correlation between microstructure and mechanical strength," *Journal of Materials Science*, vol. 40, no. 19, pp. 5249–5253, 2005.

[10] M. H. Ge, *Research on Current Situation and Comprehensive Utilization of Straw Resources in Jilin Province*, Master thesis of Northeast Normal University, 2011.

[11] H. Liu, L. M. Zhang, and N. Q. Wang, "Research on current situation and development of straw panel," *China New Technologies and New Products*, vol. 2014, no. 5, p. 131, 2014.

[12] G. H. Chen, "Study on surface properties and gluing re-
combination technology of crop straw," Master thesis, of
Central South University of Forestry and Technology,
Changshu, China, 2006.

[13] C. Martins, A. M. P. G. Dias, and H. Cruz, "Bonding per-
formance of Portuguese Maritime pine glued laminated
timber," *Construction and Building Materials*, vol. 223,
pp. 520–529, 2019.

[14] X. Li, Z. Cai, and J. Z. Winandy, "Effect of oxalic acid and
steam pretreatment on the primary properties of UF-bonded
rice straw particleboards," *Industrial Crops and Products*,
vol. 33, no. 3, p. 665~669, 2012.

[15] J. A. Newlin and J. M. Gahagan, "Tests of large timber col-
umns and presentation of the forest products laboratory
column formula," United States Department of Agriculture,
Washington. D.C, USA, Technical Bulletin No.167, 1930.

[16] B. Sharma and K. A. Harries, "Effect of fiber gradation on the
edge bearing strength of bamboo culms," *Key Engineering
Materials*, vol. 517, pp. 63–70, 2012.

[17] T. Reynolds, B. Sharma, K. Harries, and M. Ramage, "Dowelled
structural connections in laminated bamboo and timber,"
Composites Part B: Engineering, vol. 90, pp. 232–240, 2016.

[18] J. J. Zahn and D. R. Rammer, "Design of glued laminated
timber columns," *Journal of Structural Engineering*, vol. 121,
no. 12, pp. 1789–1794, 1995.

[19] Z. Li, M. He, D. Tao, and M. Li, "Experimental buckling
performance of scrimber composite columns under axial
compression," *Composites Part B: Engineering*, vol. 86,
pp. 203–213, 2016.

[20] P. Luna, C. Takeuchi, C. Alvarado, and I. Moreno, "Glued
laminated Guadua angustifolia bamboo columns," in *I In-
ternational Symposium on Genetic Resources of Bamboos and
Palms and III International Symposium on Ornamental
Palms* vol. 1003, pp. 125–130, 2013.

[21] H.-t. Li, J.-W. Su, Q.-S. Zhang, A. J. Deeks, and D. Hui,
"Mechanical performance of laminated bamboo column
under axial compression," *Composites Part B: Engineering*,
vol. 79, pp. 374–382, 2015.